Journal of Zhejiang University-SCIENCE A (Applied Physics & Engineering)
ISSN 1673-565X (Print); ISSN 1862-1775 (Online)
www.jzus.zju.edu.cn; www.springerlink.com
E-mail: jzus@zju.edu.cn

Variable bead width of material extrusion-based additive manufacturing*

Jun WANG[1], Ting-wei CHEN[1], Yu-an JIN[†‡1,2,3], Yong HE[2]

[1]*School of Mechanical Engineering and Mechanics, Ningbo University, Ningbo 315211, China*

[2]*School of Mechanical Engineering, Zhejiang University, Hangzhou 310027, China*

[3]*Key Laboratory of Advanced Manufacturing Technology of Zhejiang Province, Hangzhou 310027, China*

[†]E-mail: jinyuan@nbu.edu.cn

Received May 4, 2017; Revision accepted Nov. 1, 2017; Crosschecked July 10, 2018; Published online July 25, 2018

Abstract: Variable bead width in material extrusion-based additive manufacturing (MEAM) is studied to enhance flexibility and capability. Discussion on associated process parameters, including the layer thickness, material flow rate, and travel feed rate is conducted to deduce their potential influence on the bead width of deposited filaments. Then the analytical models are established to analyze their effects on the bead width quantitatively. Based on the theoretical and experimental analyses, the material extrusion flow rate is selected as the input variable to control the bead width during the extrusion and deposition processes. The proposed method is implemented and verified with deposition of a multi-layer but single column thin-walled structure. Based on the implementation of several applications, it is concluded that the bead width could be achieved by adjusting some related process parameters and it can facilitate the extension and application of extrusion-based additive manufacturing technology.

Key words: Extrusion-based additive manufacturing; Variable bead width; Process parameters; Analytical models; Experimental applications

https://doi.org/10.1631/jzus.A1700236 **CLC number:** TH161.12

1 Introduction

Material extrusion-based additive manufacturing (MEAM) represented by fused deposition modeling (FDM) has become one of the most widespread additive manufacturing (AM) techniques because of its flexibility, extensibility, implementation simplicity, and enhanced capability in fabricating parts, without any geometrical limitations, directly from the digital file of the desired models (Turner et al., 2014). In comparison with conventional subtractive manufacturing paradigms, it has the ability to rapidly fabricate parts with variable material distribution and complex geometries within a reasonable time and cost using a variety of materials, including thermoplastics, ceramics, bio-compatible hydrogels, silicones, and concretes. Hence, this technology has been widely applied in various fields, such as the prototype fabrication, biomedical industry, construction, and consumer market. However, this technology itself still has some drawbacks and limitations, such as poor surface roughness due to the staircase effect and relatively long build time that severely affects the further application of additively fabricated parts.

The issues related to surface roughness and build time have been investigated via building theoretical models from which some process parameters are selected to be optimized. With respect to surface

‡ Corresponding author

* Project supported by the Natural Science Foundation of Zhejiang Province (No. LQ18E050004), the Initial Foundation of Ningbo University (No. 421610040), and the K. C. Wong Magna Fund in Ningbo University, China

ORCID: Yu-an JIN, https://orcid.org/0000-0003-3775-6162

roughness, Rahmati and Vahabli (2015) presented several analytical models to express the surface roughness distribution in FDM and the models were evaluated according to the variations of surface build angle. Furthermore, they proposed an accurate model to estimate surface quality in the process planning stage to optimize some parameters. Ahn et al. (2009) introduced a new approach to model the surface roughness of FDM-fabricated parts by considering some key variables determining the section shape of the extruded filament on the basis of some investigations of the actual surface profile of the part. To improve surface quality, many methods were developed to post-process the fabricated part, including chemical (McCullough and Yadavalli, 2013; Jin et al., 2017a) and physical strategies (Boschetto et al., 2016). As for build time reduction, Zhu et al. (2016) established an analytical model to theoretically analyze the factors that affect the part built time and used this model to facilitate the design of the parts for parameter optimization.

The above models and methodologies are commonly easily implemented and achieved in the MEAM system because of its flexibility and extensibility in the process planning stage (Kulkarni et al., 2000). Process planning plays a role as a bridge between 3D models and AM machines by transferring the digital models into codes that can be read by the hardware. Four main steps are involved in the process planning of MEAM: orientation determination, support generation, slicing, and extruder path planning (Fig. 1) (Jin et al., 2015b). In general, the path space in the path generation step is supposed to be a certain value based on the assumption that the deposited bead width is unchanged. However, this is not always the case in practical fabrication.

It is understandable that the bead width of deposited filaments can change slightly when some parameters are changing in the fabrication process (Jin et al., 2017b) which will be further studied. There have been some studies on the cross-sectional shape of the deposited filament that involves the bead width, mainly for modeling the surface profile of AM-fabricated parts. Ding et al. (2016) adopted an artificial neural network to establish the relationship between the bead model and welding parameters in the wire and arc AM. A multi-bead overlapping model called 'tangent overlapping model' was built to obtain the critical center distance for stable multi-bead overlapping processes (Ding et al., 2015). Li et al. (2007) proposed a modified multi-gene genetic programming method using a stepwise regression approach to study the bead width data obtained from experiments and the performance of the model was evaluated on the stereolithography (SLA) machine. However, as far as we know, there has been little systematic and quantitative work on the influence on the bead width from process parameters in this field.

In MEAM, there are a variety of process parameters affecting the performance of fabricated parts (e.g. surface roughness, dimensional accuracy, and mechanical property) and the fabricating process. To facilitate the distinction, the process parameters are categorized into two groups of pre-process parameters (PPPs) and fabricating process parameters (FPPs) based on the applied phase during the whole AM process according to our previous study (Jin et al., 2015a). The former group of parameters usually appears in the process planning stage and would not be modified during the fabricating process. These include building direction, layer thickness, maximal self-support angle, path gap, and inclination, while the latter group occurs in the real-time fabricating process, including material flow rate Q and feed rate f. Both groups of parameters would affect the bead width of deposited filaments from different perspectives.

This study aims at the formulation of the relationship between the bead width and process parameters. The analytical models are established through several sets of experiments and the key parameters are selected as the input variables to control the bead width of deposited filaments. The models are implemented and evaluated with a multi-layer but single-column thin-walled structure. Finally, three applications of variable bead width are provided to further verify the significance and purpose of this research.

2 Variable bead width

In the practical extrusion and deposition process of MEAM, the feed rate is variable because of sharp corners and high curvature segments along the deposition path. At corners, the feed rate is supposed

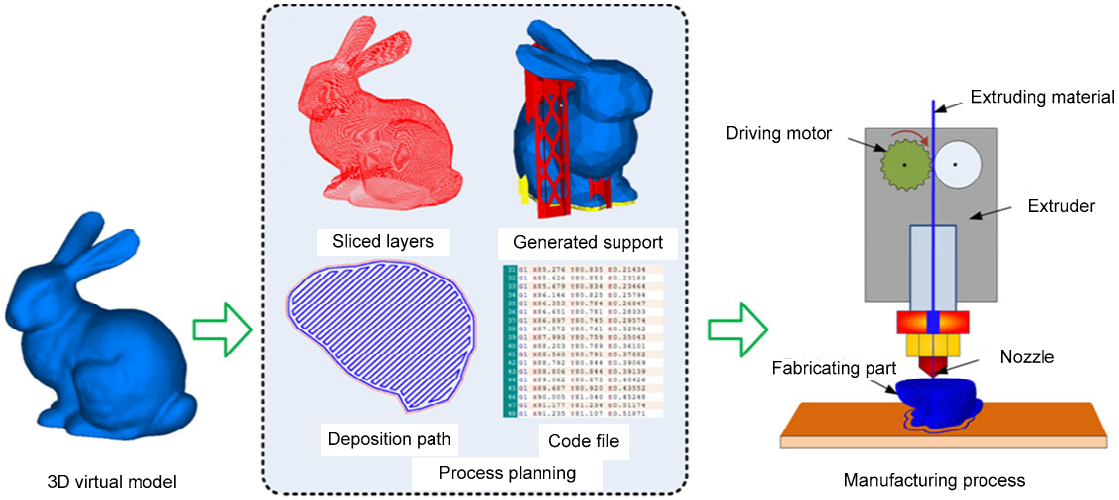

Fig. 1 An illustration of the process planning in MEAM
Manufacturing process is cross-section from (Jin et al., 2015b)

to be reduced to transit smoothly, so the material flow rate should also decrease. Based on this, the bead width, associated with the cross-section of deposited filaments, can be controlled by adjusting the proportion between the material flow rate and the travel feed rate. This is the foundation for modeling the bead width.

To provide a benchmark for modeling the bead width, several associated process parameters are discussed in terms of their relationship with the bead width based on current research results. The first parameter is the layer thickness, which is the thickness of slices during the slicing and fabricating procedure. The sliced layers approximate the original 3D models and the resolution is determined by the layer thickness. Layer thickness and bead width are two key parameters in determining the cross-section of deposited filaments and play an important role in the inner strength and surface profile of fabricated parts. In most cases, the layer thickness is decided by the resolution requirement and the cross-section of the deposited filament is shaped by the mechanical interaction between the nozzle tip and the extruded materials.

In addition, the proportion between material flow rate Q and nozzle feed rate f determines the extruded material volume per unit length along the planned deposition path. In other words, the flow rate must be adjusted when the feed rate is changing in order to guarantee that the cross-section of deposited filaments remains constant. Thus, to achieve relatively uniform deposited filaments, the proportion of Q and f should theoretically be confined within a certain range.

Based on the above analysis, physical models can be established for controlling the bead width quantitatively. During the extrusion process, the material is extruded at a flow rate which is controlled by either the rotation speed of the motor in the mechanical extrusion system or the air pressure in the pneumatic extrusion system. The extruded materials are deposited and distributed along the deposition path depending on the travel feed rate of the nozzle. The cross-sectional area of deposited filaments can be obtained by Eq. (1) based on the law of conservation of volume:

$$s=\frac{Q}{f}. \tag{1}$$

The detailed description on the cross-section has attracted much attention and several geometric models have been built (Boschetto et al., 2012; Ding et al., 2016). The difficulty in modeling the cross-sectional shape is identifying the function to represent its profile. In Fig. 2, three cases with different layer thicknesses (t) are selected with the material extrusion flow rate and the travel feed rate kept constant at 2.5 mm^3/s and 25 mm/s, respectively and the layer thickness varying from 0.3 mm to 0.2 mm. The top and bottom

surfaces of deposited filaments are shaped by mutual compression and tend to be flat; the edge of deposited filaments cannot be compressed flat and its shape depends on the area of the cross-section and the layer thickness. From the cross-sections under different layer thicknesses in Fig. 2, we can observe that the edges of filaments do not always have the same geometry and it is hard to use one uniform function to express them.

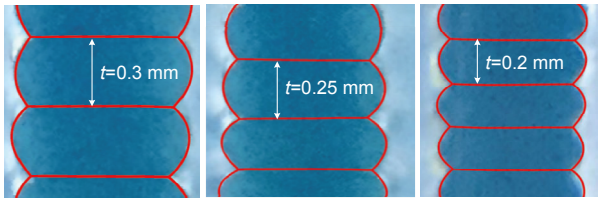

Fig. 2 Illustration of deposited filament's cross-section under different layer thicknesses

In this study, the bead width (w) is defined as the total length of the cross-section of deposited filaments (Fig. 3). Without considering the detailed shape of the cross-section, the cross-sectional area s can be expressed as

$$s = tw\eta, \tag{2}$$

where η is the coefficient to approximate the equivalent width for calculating the cross-sectional area, $\eta<1$. The value of η is variant depending on some associated process parameters and the material itself. Thus, it is important to determine η to obtain the bead width in studying the influence of the related process parameters on the bead width. Each geometric model of the cross-sectional shape would have a specific expression for the coefficient η. Using the geometric model of FDM fabricated parts developed in our previous study (Jin et al., 2015a), η can be expressed as Eq. (3), which is adopted to calculate the reference value of η_o.

$$\eta = \frac{(w-t)t + \pi(t/2)^2}{tw}. \tag{3}$$

To investigate the factors that affect the bead width from Eqs. (1)–(3), three groups of experiments are designed and conducted. The FDM printer used in this study is Lulzbot TAZ3 with polylactic acid (PLA) as extruded material. The format of the Gcode is open

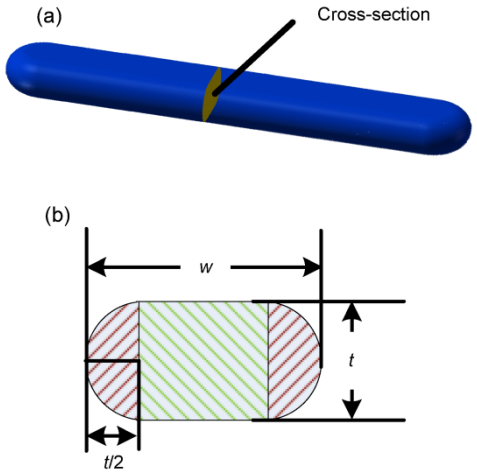

Fig. 3 Illustration of the cross-section of deposited filament

(a) Deposited filament; (b) Detailed cross-sectional shape

source and all the Gcodes are generated with process planning software for 3D printing developed by our research group using the C++ programming language. A single-column walled model (8 mm long) is adopted in each group to obtain the cross-sections by cutting the fabricated parts vertically. The total number of layers is 10 regardless of the layer thickness, which means the model height is not necessarily uniform.

In the first group, the flow rate and the feed rate are kept constant at 2.5 mm^3/s and 25 mm/s, respectively, and the layer thickness is variable. The cross-sectional area s is the same in theory since Q and f are unchanged in each test and the bead width is obtained and measured using an optical microscope. The area of each cross-section should be 0.1 mm^2 according to Eq. (1). Fig. 4 shows the experimental results. As can be observed from the figure, the measured bead width has the same tendency as the equivalent bead width as expected. Then, the coefficient η can be calculated by dividing the equivalent bead width by the measured value. For comparison, the reference value η_o from Eq. (3) is also displayed and good agreement between them is shown.

At the same time, we can see that η decreases gradually when the layer thickness increases. An interesting observation is that the coefficient η is smaller than η_o when the layer thickness is small, while the gap becomes smaller and η transfers to be larger than η_o when t exceeds a certain value (0.2 mm in the figure). The reason behind this observation is that the extruded materials are squeezed towards the

outside and the cross-sectional edge with a smaller thickness tends to be sharper than that under a larger layer thickness. This can be verified from the captured photos in Fig. 4.

In the following two groups of tests, the flow rate Q and feed rate f are the variables. In the first group, the layer thickness is set at 0.2 mm, and the feed rate is 25 mm/s. As the feed rate varies during the deposition process, especially at the start or the end point of the path segment, the cross-section to be measured is chosen at the intermediate part of the deposited walled part to ensure that the feed rate at the chosen point is at the expected value. In this group, the material extrusion flow rate is controlled by adaptively setting the displacement of the motor within a certain length of the deposited path.

Fig. 5 shows a linear relation between the measured bead width and the material flow rate. This agrees with the tendency of the equivalent bead width w_o obtained from Eq. (2). As the layer thickness is the same in each test, the profiles of the cross-sectional edge are similar, leading to the coefficient η floating up and down along the line representing the reference value of η_o. Hence, it can be concluded that the established geometric model representing the surface profile of deposited filaments is feasible in our previous study (Jin et al., 2015a) when the layer thickness is 0.2 mm approximately. It should be noted that the bead width is not available to be measured when the flow rate is 1.2 mm^3/s. That is because the diameter of the nozzle tip is 0.35 mm and such a small flow rate would result in a discontinuous deposited filament. Thus, the flow rate needs to be within a certain range to form continuous and desired filaments.

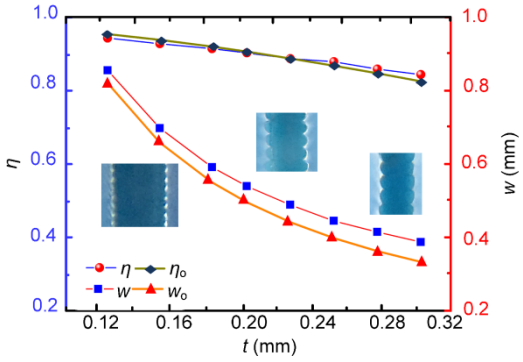

Fig. 4 Experimental results on the relation between layer thickness and the bead width with Q=2.5 mm^3/s and f=25 mm/s

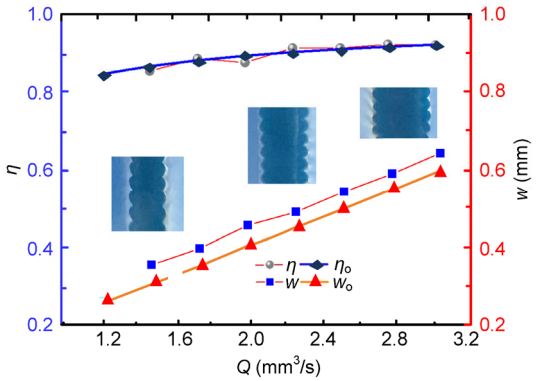

Fig. 5 Experimental results on the relation between flow rate and the bead width with t=0.2 mm and f=25 mm/s

As can be concluded from the results, the bead width can be adjusted by simply modifying the material flow rate while the travel feed rate and the layer thickness are kept constant. The linear proportional relation between them facilitates practical operation from the perspectives of both control and calculation. Therefore, the variable bead width can be realized via this strategy.

In the last group, the layer thickness is also 0.2 mm and the flow rate is constant and set at 2.5 mm^3/s. As expected, the bead width is changed when the feed rate changes and the relationship between them is expressed in Eq. (2). Likewise, the bead width and the coefficient η agree well with the reference values. However, the frequent acceleration/deceleration performance of motors along the x and y directions is not desirable in the majority of available material extrusion-based machines. The formed surface of fabricated parts usually has obvious flaws. Thus, obtaining variable bead width by frequently changing the travel feed rate is not recommended.

So far, it has been verified that a variable bead width is obtainable and controllable. Three associated process parameters, i.e. layer thickness, material flow rate, and travel feed rate, and their relationships with the bead width are investigated and analyzed. The corresponding tests have been conducted for validation of the bead width model and the results are acceptable. As the layer thickness is affected by many other factors, like fabrication efficiency and resolution requirement, it is reasonable to select the material flow rate and travel feed rate as the control variables to control bead width.

Up to now, the most desirable method to achieve variable bead width is to adjust the material flow rate for the aforementioned reasons. Since the coefficient η will change when the bead width changes, it is reasonable to use an appropriate geometrical model to express the coefficient, like the verified Eq. (3). From Eqs. (1)–(3), the bead width can be expressed as Eq. (4) considering the correlated change of coefficient η. It can be seen from Fig. 6 that the bead width is proportional to the material flow rate when the travel feed rate and the layer thickness are kept constant. This equation would be the foundation for generating variable bead width by controlling the material extrusion speed.

$$w=\frac{1}{t}\left(\frac{Q}{f}-\frac{\pi t^2}{4}\right)+t. \tag{4}$$

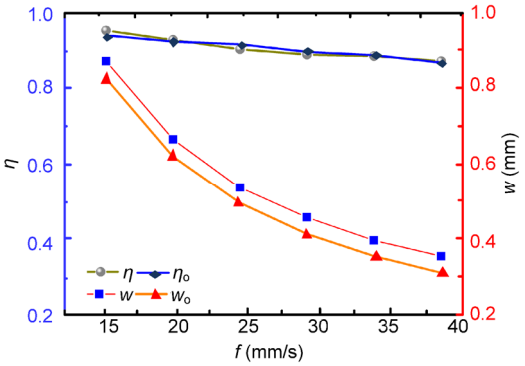

Fig. 6 Experimental results on the relation between feed rate and bead width

Fig. 7 illustrates the steps through the process planning stage and the fabrication process to generate variable bead width. In the process planning, the information on the bead width should be mapped to specific points based on the requirement first. Then, the value of the bead width is transferred to the material flow rate according to Eq. (4), and the flow rate is quantified and saved in the Gcode. In the extrusion process, the material flow rate is controlled by the rotation speed of the drive motor to achieve variable bead width.

With the proposed approach, two multi-layer single-column walled parts are deposited and their cross-sections are shown in Fig. 8. To achieve uniform resolution of the surface, the layer thickness is the same between layers and the bead width is controlled by changing the material extrusion flow rate during the deposition process. Continuous variation of the inclination can be seen from the surface of deposited parts.

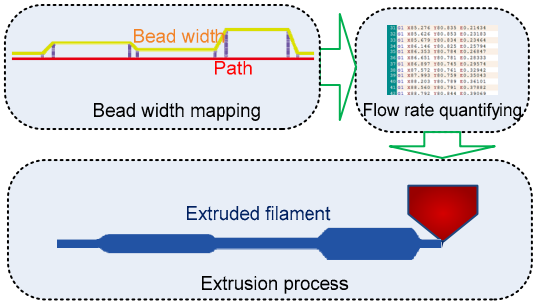

Fig. 7 Flowchart of the proposed approach

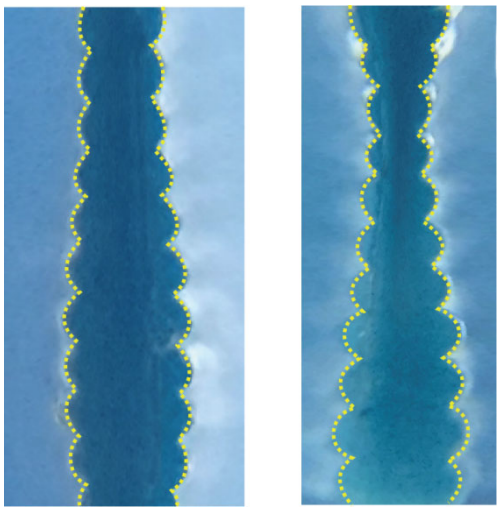

Fig. 8 Photos of two single-column walled parts with variable bead width

3 Applications

Besides the issues of surface quality and build time, there are some other intractable problems resulting from the constant bead width which need to be addressed in MEAM. For example, the underfills and overfills in filling the top surface usually appear when the total length of the area along the direction perpendicular to the planned path is not an integral multiple of the bead width (Jin et al., 2014). Second, when fabricating an inclined thin-walled part with equal thickness but with varied inclination angles, it is impossible to obtain constant wall thickness using the constant bead width due to the step effect on the side

surface when the number of the bead changes. Moreover, it is very difficult to fabricate tiny features on the thin wall no matter which build orientation is selected. Fortunately, with the knowledge on the controllable bead width proposed in this study, all these issues can be solved by adjusting the bead width on some specific layers or within some specific areas on one layer. In this section, several potential applications of the variable bead width are demonstrated and discussed.

3.1 Fabrication of tiny and critical features

It is difficult for the MEAM to fabricate components having randomly located, small-dimensioned but critical surface features on the top surface. As analyzed, the staircase effect on the top surface tends to result in the loss of some tiny features and the continuous and smooth inclined surface cannot be deposited due to the nature of flat AM. An intuitive solution to fabricate such tiny features is to use curved AM (Jin et al., 2017b), but some algorithms in the process planning of curved AM, including slicing and path generation, are complex and not easy to be extended to general MEAM systems. Fortunately, this issue can be solved by adjusting the build direction as mentioned above.

When the tiny features are located on the side surface, these features can be formed theoretically by planning the deposition path on each layer. In Fig. 9a, the part to be fabricated has an inclined thin feature on its surface; the thickness of the feature is continuously changing from 0.6 mm to 0.1 mm. If the feature is placed on the top surface, some features have been missed when the slicing thickness is set as 0.25 mm (Fig. 9b). Fig. 9c shows the corresponding fabricated part. An obvious staircase effect leads to the surface seriously deviating from the desired part. On the other hand, the tiny features are transferred to the side surface and the slicing results are shown in Fig. 9d. In planning the deposition path, the path is generated initially without considering the tiny features, and then some path segments of the original path are offset towards the edge to form the tiny features on each layer (Fig. 9f). The offset distance is the half the overhanging length. The simulated deposition result is shown in Fig. 9e and the fabricated part can restore all the tiny features perfectly (Fig. 9g).

Using the variable bead width to restore tiny features on the side surface is very useful especially when all the tiny features are located on one surface. The resolution of the fabricated tiny part on the side surface is the layer thickness while the resolution on

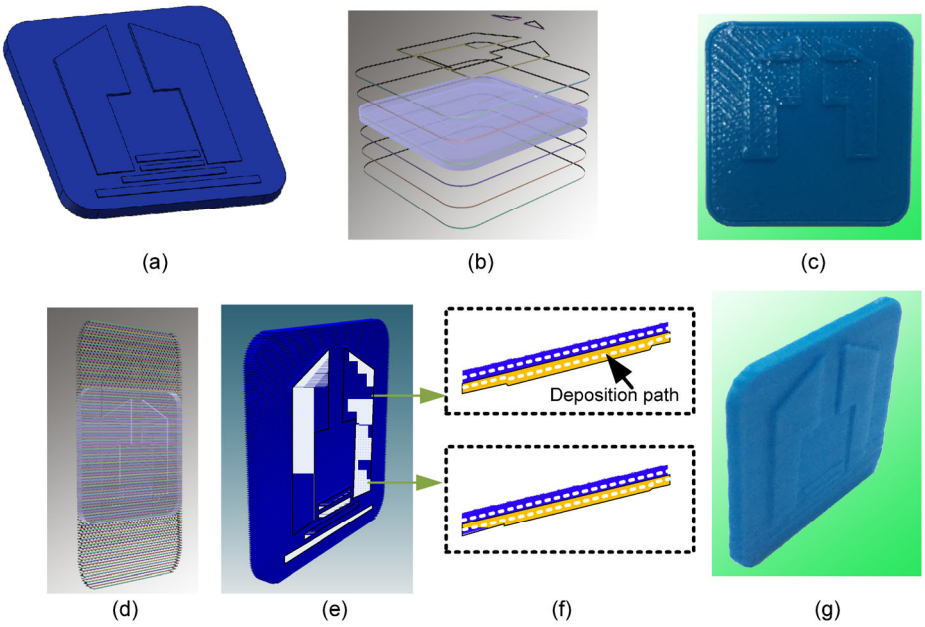

Fig. 9 Fabrication of tiny features by transferring from top surface to side surface

(a) Part to be fabricated; (b) Slicing based on original build direction; (c) Fabricated part 1; (d) Slicing based on adjusted build direction; (e, f) Design of deposition parameters; (g) Fabricated part 2

the top surface is the bead width. For the FDM printer in our study, the layer thickness can reach a minimum value of 0.07 mm while the bead width cannot go smaller than the diameter of the nozzle tip (0.35 mm generally). Hence, the obtainable resolution of features on the side surface is higher. Note that the bead width cannot go beyond a certain value as reported in the last section, so the formed features should have a limited size.

3.2 Improvement of filling quality

In MEAM systems, the deposition quality is mainly dependent on the distribution of materials, involving the layout of deposition paths and the material volume per unit length along the path. Many strategies have been developed to improve the evenness of the deposited surface by obtaining uniform gaps between path segments. In theory, desirable filling quality can be achieved if the whole area is covered with uniform gaps and the deposited bead width is also uniform. However, there are no available path planning strategies satisfying this requirement in processing any contours which commonly contain a variety of arbitrary geometries. Thus, deposition quality resulting from this is one of the intractable issues needing to be addressed.

Here, the total area of voids and overfills resulting from improper gaps between adjacent paths can be used to quantify the filling quality. If the bead width is uniform, voids and overfills are unavoidable when the path gap does not suit the width of the deposited beads. However, this issue can be alleviated to some extent using a variable bead width. Specifically, the path gap can be adaptively adjusted within a certain range in the path planning stage to cover the whole area and then the bead width is controlled to fill the gaps along the path evenly and to avoid voids and overfills. For example, the contour parallel-based path is used to fill a surface shown in Fig. 10a, with the path generated with a constant gap without considering the bead width and the geometric characteristics of the shape. From Fig. 10c, in addition to some small valleys between adjacent path segments because of insufficient filling, several large voids appear in the interior of the part because of the inherent property of the contour-parallel-based path pattern. To avoid serious internal voids, the path planning strategy proposed by Ding et al. (2016) is adopted to generate the filling path (Fig. 10b). The distance between adjacent path segments is adaptively changed to ensure that the path gap is limited to a certain range and is as uniform as possible. The deposition result is shown in Fig. 10d where the bead width is kept constant based on the generated filling path. The deposition quality is fairly good in some areas where the path gap and the bead width match with each other, while some valleys still exist when the path gap is larger than the bead width. However, these small valleys can be completely avoided using the variable bead width (Fig. 10e). The bead width is supposed to be enlarged at the areas properly based on the distance between adjacent segments to achieve satisfied deposited surface. Thus, improving the filling quality in the MEAM process is one of the biggest advantages of the variable bead width used as a strategy in the path planning stage.

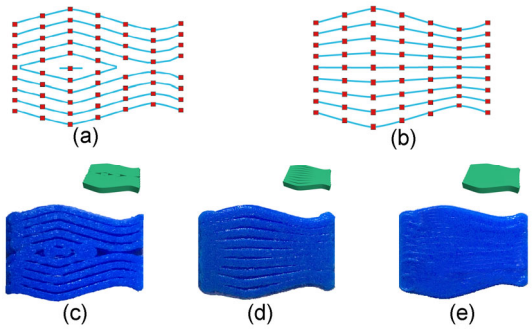

Fig. 10 Influence on the deposition quality of variable bead width

(a) Contour parallel paths; (b) Optimized paths; (c) Deposition result using paths in (a); (d) Deposition result using paths in (b) with uniform bead width; (e) Deposition result using paths in (b) with variable bead width

3.3 Self-support enhancement

In the AM process, an overhanging region that can be fabricated without additional support is called as self-supported (Hu et al., 2015). The angle between the region's tangent plane and the building direction is called the self-support angle θ (Fig. 11b). The maximal self-support angle θ_{max} is the threshold value of the self-support angle which means if θ is smaller than θ_{max}, the surface can be fabricated successfully without adding support (Fig. 11c). The surface within the circle can be called a self-support area, while the surface outside this area cannot be built without support. The maximal support angle is dependent on

the materials used, the bead width, and the layer thickness. With a given t and w, θ can be expressed as

$$\theta=\arctan\left(\frac{\tau w}{t}\right), \tag{5}$$

where τ is the ratio between the overhanging length and the bead width.

From Eq. (5), the overhanging length is affected by not only the material properties but also the bead width and layer thickness, and thus can be controlled by modifying these parameters.

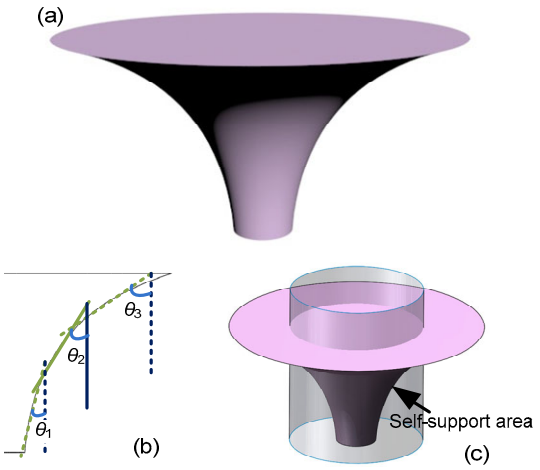

Fig. 11 Illustration of the maximal self-support angle
(a) A part surface with variant surface inclination; (b) Self-support angles; (c) Self-support area

As mentioned, the maximal self-support angle is considered as a critical parameter in deciding whether the support structures are required. Increasing the maximal self-support angle is an effective approach to reducing the demand for support structures and then avoiding the harm brought about by the support, like the material consumption, poor surface finish, and post processing. Although the maximal self-support angle is largely affected by the material properties, the bead width is also an important factor. Specifically, the overhanging length of the outmost deposited bead can be increased slightly under a certain layer thickness when the bead width increases.

Taking the part in Fig. 11a as an example, two experiments are designed to compare the maximal self-support angle and work out the influence on self-support capability of the bead width. In both experiments, the layer thickness is the same and the bead width is also unchanged in the first experiment (Figs. 12a and 12b), while the bead width of the outmost filament is designed to be larger than that of internal filaments in the second experiment (Figs. 12d and 12e). We can see that the edges of both fabricated parts are distorted and wrapped without the assistance of support structures. However, the self-support ability is obviously enhanced with a larger bead width (Figs. 12c and 12f). Note that a larger bead width can indeed improve the maximal self-support angle, but fabrication resolution is also weakened. So the variable bead width can satisfy these two requirements perfectly.

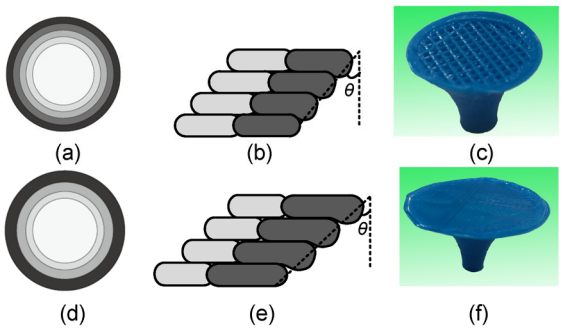

Fig. 12 Influence on the maximal self-support angle of variable bead width
(a) Uniform bead width; (b) Maximal self-support angle with (a); (c) Fabricated part with uniform bead width; (d) Variable bead width; (e) Maximal self-support angle with (d); (f) Fabricated part with variable bead width

4 Conclusions

In this study, the variable bead width of deposited filaments in material extrusion-based AM was investigated both theoretically and experimentally. Based on the theoretical analysis, the relationship with the bead width of layer thickness, material flow rate, and travel feed rate were studied. The experimental results verified the analytical models and showed that the material extrusion flow rate was effective for controlling the bead width within a certain range. With the variable bead width, many potential applications can be realized and three cases were reported, including the fabrication of tiny features on the side surface, improving the filling quality, and enhancing the self-support capability. This method of achieving variable bead width in MEAM can be easily extended and adopted for different materials either to improve part performance or even to solve issues resulting from the constant bead width.

References

Ahn D, Kweon JH, Kwon S, et al., 2009. Representation of surface roughness in fused deposition modeling. *Journal of Materials Processing Technology*, 209(15-16):5593-5600.
https://doi.org/10.1016/j.jmatprotec.2009.05.016

Boschetto A, Giordano V, Veniali F, 2012. Modelling micro geometrical profiles in fused deposition process. *International Journal of Advanced Manufacturing Technology*, 61(9-12):945-956.
https://doi.org/10.1007/s00170-011-3744-1

Boschetto A, Bottini L, Veniali F, 2016. Finishing of fused deposition modeling parts by CNC machining. *Robotics and Computer-Integrated Manufacturing*, 41:92-101.
https://doi.org/10.1016/j.rcim.2016.03.004

Ding D, Pan Z, Cuiuri D, et al., 2015. A multi-bead overlapping model for robotic wire and arc additive manufacturing (WAAM). *Robotics and Computer-Integrated Manufacturing*, 31:101-110.
https://doi.org/10.1016/j.rcim.2014.08.008

Ding D, Pan Z, Cuiuri D, et al., 2016. Bead modelling and implementation of adaptive MAT path in wire and arc additive manufacturing. *Robotics and Computer-Integrated Manufacturing*, 39:32-42.
https://doi.org/10.1016/j.rcim.2015.12.004

Hu K, Jin S, Wang CCL, 2015. Support slimming for single material based additive manufacturing. *Computer-Aided Design*, 65:1-10.
https://doi.org/10.1016/j.cad.2015.03.001

Jin Y, He Y, Xue G, et al., 2014. A parallel-based path generation method for fused deposition modeling. *The International Journal of Advanced Manufacturing Technology*, 77(5-8):927-937.
https://doi.org/10.1007/s00170-014-6530-z

Jin Y, Li H, He Y, et al., 2015a. Quantitative analysis of surface profile in fused deposition modelling. *Additive Manufacturing*, 8:142-148.
https://doi.org/10.1016/j.addma.2015.10.001

Jin Y, He Y, Fu J, 2015b. Support generation for additive manufacturing based on sliced data. *The International Journal of Advanced Manufacturing Technology*, 80(9-12):2041-2052.
https://doi.org/10.1007/s00170-015-7190-3

Jin Y, Wan Y, Zhang B, et al., 2017a. Modeling of the chemical finishing process for polylactic acid parts in fused deposition modeling and investigation of its tensile properties. *Journal of Materials Processing Technology*, 240:233-239.
https://doi.org/10.1016/j.jmatprotec.2016.10.003

Jin Y, Du J, He Y, et al., 2017b. Modeling and process planning for curved layer fused deposition. *The International Journal of Advanced Manufacturing Technology*, 91(1-4):273-285.
https://doi.org/10.1007/s00170-016-9743-5

Kulkarni P, Marsan A, Dutta D, 2000. A review of process planning techniques in layered manufacturing. *Rapid Prototyping Journal*, 6(1):18-35.
https://doi.org/10.1108/13552540010309859

Li P, Ji S, Zeng X, et al., 2007. Direct laser fabrication of thin-walled metal parts under open-loop control. *International Journal of Machine Tools and Manufacture*, 47(6):996-1002.
https://doi.org/10.1016/j.ijmachtools.2006.06.017

McCullough EJ, Yadavalli VK, 2013. Surface modification of fused deposition modeling ABS to enable rapid prototyping of biomedical microdevices. *Journal of Materials Processing Technology*, 213(6):947-954.
https://doi.org/10.1016/j.jmatprotec.2012.12.015

Rahmati S, Vahabli E, 2015. Evaluation of analytical modeling for improvement of surface roughness of FDM test part using measurement results. *International Journal of Advanced Manufacturing Technology*, 79(5-8):823-829.
https://doi.org/10.1007/s00170-015-6879-7

Turner BN, Strong R, Gold SA, 2014. A review of melt extrusion additive manufacturing processes: I. Process design and modeling. *Rapid Prototyping Journal*, 20(3):192-204.
https://doi.org/10.1108/RPJ-01-2013-0012

Zhu Z, Dhokia V, Newman ST, 2016. A new algorithm for build time estimation for fused filament fabrication technologies. *Proceedings of the Institution of Mechanical Engineers, Part B: Journal of Engineering Manufacture*, 230(12):2214-2228
https://doi.org/10.1177/0954405416640661

中文概要

题　目： 面向材料挤出成型增材制造的自适应丝宽研究

目　的： 材料挤出成型增材制造技术在成形质量与加工效率方面仍有很大的提升空间。本文通过探究成形过程中的关键参数（打印速度和施加气压）对挤出丝宽的影响，研究实现可变丝宽的方法，提出自适应丝宽在提升工艺方面的应用，从而提高该工艺的适用性。

创新点： 1. 通过实验与物理模型结合的方法，推导关键参数与丝宽的函数关系；2. 基于增材制造技术的工艺特点，提出自适应丝宽在该工艺中的典型应用。

方　法： 1. 通过物理模型分析与数学推导，构建挤出丝宽与关键过程参数的函数关系，得到众多过程参数中对丝宽影响最为显著的两个参数；2. 通过实验分析与对比，对构建的数学模型进行验证；3. 提出自适应可变丝宽的实现方法及典型应用的实施方案。

结　论： 1. 挤出成型增材制造技术可以通过参数调节获得可控的挤出丝宽；2. 两大关键工艺参数与丝宽之间存在关联函数；3. 运用自适应可变丝宽可以提高工艺的适用性。

关键词： 挤出成型；工艺参数；可变丝宽；典型应用